REAL-TIME THREE DIMENSIONAL THERMAL-HYDRAULIC INFORMATION FOR LARGE PWR CORES

Eduardo L. Cabral* and John E. Meyer

Massachusetts Institute of Technology
* Currently E. L. Cabral is at
Instituto de Pesquisas Energeticas e Nucleares - IPEN

SUMMARY

A fast running computer model that provides three-dimensional thermal-hydraulic information for a PWR core has been developed and validated. The core fluid model is based on a multi-channel approach following the assumptions of no cross-flow between channels and uniform inlet mass velocity. These assumptions were extensively studied using a complex three-dimensional code. The core fuel and conduction model provides for variations in fuel conductivity and gap conductance because of thermal effects, fuel relocation, and cracking. The core model has been coupled with models of primary loop and steam generator. The complete model is validated against real plant data over different operating transients. Execution speed of the model appears to be fast enough to achieve real-time execution on plant process computers.

INTRODUCTION

Major efforts are being made to improve the operation of nuclear power plants by developing a variety of new digital computer capabilities. Important operation aspects like power distribution control and the strong non-linear dynamics of a PWR have to be addressed for a successful automation of a PWR power plant. A fast running computer model that provides three-dimensional thermal-hydraulic information of a pressurized water reactor (PWR) core has been developed and validated. This model is to provide input for reactivity feedback calculation for a fast running three dimensional calculation of core power distribution [1]. The thermal-hydraulic core model must describes both the fuel and coolant conditions under normal conditions of operation. The core model has been coupled with models of primary loop and steam generator to aid in simulating real plant data.

The above models have a variety of applications in power plant technology. They can be incorporated in a automatic controller for power and power distribution. The models can be used as part of a Safety Parameter Display System (SPDS). The models can also be used to provide information in signal validation efforts and in fault detection and identification (FDI) systems. All these functions require fast running models with a certain degree of complexity. In addition, these models coupled with other component models (pressurizer, pump and complete secondary system) can be used for operation training and as an aid for operation.

There are many faster-than-real-time digital simulation models for PWRs. However, they typically use only ten or fewer control volumes to represent the entire reactor coolant system and are based on a single phase formulation. A summary of these codes can be found in [2]. Little work exists relevant to real-time, three dimensional, thermal-hydraulic modeling of PWR cores.

Concerning coolant conditions, much of the recent work in core modeling involves complex and detailed, three dimensional representation of fluid behavior, such as COBRA [3] and THERMIT [4]. In general these models include also some description of the heat conduction in the fuel. However, they do not include important effects such as fuel relocation and cracking. The most relevant, if not the only work with respect to real-time, three dimensional modeling of the reactor core is a less detailed computer model, which was developed by Chiu [5]. Chiu's model was aimed at simulating conditions for calculating thermal safety margins during normal operation. However, the model assumes a steady-state condition and it is not complete in the sense that it does not consider heat conduction in the fuel.

Several works exist that deal with detailed description of the thermal phenomena in the fuel of light water reactors, such as fuel relocation and cracking. However, these studies are usually associated with reactor safety and fuel performance rather than with accurate three-dimensional modeling. Maki [6] performed a very good compilation and comparison of many fuel relocation and cracking models.

CORE FLUID MODEL

The necessity of providing input for a three dimensional calculation of core power distribution imposes a certain degree of complexity in the model which can be incompatible with the requirements of a real-time calculation. Thus, the following simplified assumptions have been made:

- the model is based on flow channels of the size of one or more physical fuel assemblies;
- cross flow between channels is not considered;
- the inlet mass velocity is the same for all channels; and
- the momentum equation is not considered (a spatially uniform pressure is assumed).

The simplified assumptions of no cross flow and uniform inlet mass velocity were extensively studied in order to verify the restrictions and degree of precision of the resulting model. This study was based on the simulation, with the computational code THERMIT-2 [4], of nine adjacent fuel assemblies, representing both the hot and the cold portion of a 3411 MW PWR core. To isolate and evaluate separately each one of the two assumptions three different modeling approaches for these nine assemblies were used:

(1) No cross flow and specified inlet velocity;
(2) Cross flow is allowed and inlet velocity is specified; and
(3) Cross flow is allowed and a pressure drop boundary condition is used (the inlet velocity for each flow channel is a calculated result).

Several steady-state and transients were simulated. Tables 1 and 2 present a summary of the results, more detailed results and information about the simulation conditions can be obtained in [7]. In this tables, the maximum error between the different modeling approaches is given for nodal temperature, quality, and inlet velocity. The radial power distributions used are shown in Figure 1. The distributions for the hot and the cold portions are typical for a large PWR and were obtained from [8]. The third distribution used in some transients is hypothetical and presents power peaks much greater than the usually found in normal PWRs.

It can be seen from Tables 1 and 2 that the assumptions of no cross flow and uniform inlet mass velocity are extremely good. For the steady-state cases, where the power distribution is inside the normal limits, the errors are very small both for the temperature and for quality. For the transient cases with no change of radial power distribution and with change of radial power distribution from hot to cold, the errors are the same as for the steady-state cases. For the transients with change to the hypothetical radial power distribution the errors are larger. However, these errors are caused by the large difference in radial power. The transient of power increase to 120% with change to the hypothetical radial power distribution can be viewed as a limiting condition were the two assumptions begin to be questionable.

In conclusion, a model that considers neither cross flow nor flow split among channels can be very accurate for normal and near normal conditions of operation. These conditions are defined as follows: a) no substantial boiling inside the core and b) radial power ratios between assemblies (or channels) not much greater than one (e.g. 1.6).

Table 1
Summary of Steady-State Results of Assessment of Basic Fluid Model Assumptions

Steady-State	Maximum Error		
	Inlet Vel. (m/s)	Temperature (^{o}C)	Quality (%)
Hot Assemblies at 100% power	0	0.2	-
Cold Assemblies at 100% power	0	0.1	-
Hot Assemblies at 120% power	0	0.2	0.01
Hot Assemblies 100% power and 10% less flow	0	0.2	0.04

Table 2
Summary of Transient Results of Assessment of Basic Fluid Model Assumptions

Transient	Maximum Error		
	Inlet Vel. (m/s)	Temperature (^{o}C)	Quality (%)
Step in power to 120%	0	0.2	0.01
Same as before with change to hypothetic dist.	0	1.6	2.0
Same as before with change to cold power dist.	0	0.2	0.01
Change to hypothetical/ power dist.	0	0.4	0.37
Step in Power to 75%	0	0.2	-

Note: Initial condition for all these transients is reactor at 100% of power and with the hot radial power distribution.

1.153	1.189	1.153
1.212	1.152	1.208
1.137	1.191	1.128

Power Distribution of the Hot Portion of the Core

1.068	1.257	0.931
1.093	0.931	0.995
0.992	0.840	0.471

Power Distribution of the Cold Portion of the Core

1.5	1.1	1.0
1.4	1.3	0.9
0.7	0.8	0.7

Hypotetical Power Distribution

Fig. 1: Radial Power Distributions Used for the Study of Basic Assumptions of the Core Fluid Model

Governing Equations. Since conservation equations for fluids and their solution are extensively treated in the literature only the basic equations are presented here (more detail derivation can be found in [7]). The mass and energy balance for the fluid are:

$$A\frac{\partial}{\partial t}\rho + \frac{\partial}{\partial z}\dot{m} = 0, \qquad (1)$$

$$A\frac{\partial}{\partial t}\rho h + \frac{\partial}{\partial z}\dot{m}h = q_c A + q''_w P_w, \qquad (2)$$

where ρ is the fluid density, h is the flowing enthalpy, $\dot{m}$ is the mass flow rate, q_c is the volumetric heat deposition rate in the coolant, q''_w is the wall heat flux, A is the flow area, and P_w is the heated perimeter. Note that the average enthalpy is assumed to be equal to the flowing enthalpy.

The above equations are applied to a number of parallel independent channels, each channel representing one or more physical fuel assemblies. By dividing each channel into a finite number of axial segments and assigning the main variables specific positions on the resulting computational mesh, the partial derivatives in space are approximated by finite differences. The donor cell approach is used for the convective terms in the energy equation and the time derivatives are approximated by first-order backward differences, resulting then, in implicit difference equations.

The model also provides for subcooled and nucleate boiling. The model for subcooled void fraction, which is based on a correlation for the point of bubble departure, on a fit-void profile (exponential function) and on a slip ratio correlation, was checked reasonable well against Maurer's [9], Egen's [10] and Martin's [11] experimental data. Reference [7] is recommended for more details.

CORE FUEL MODEL

Accurate calculations of fuel rod temperatures are required both to find the heat transfer from the fuel to the coolant and to determine reactivity feedback calculation. Reliable estimates must be incorporated for many major effects, including fuel-to-cladding gap conductance, fuel and cladding thermal conductivity versus temperature, and influences of cracking. Two radial fuel nodes are used to calculate fuel and cladding temperatures in each control volume.

Two-Node Fuel Rod Heat Conduction Model. The solution of the radial heat conduction in the fuel pellet and cladding is formulated by a integral method which uses defined temperature profiles for the fuel and for the cladding. This is expected to give results as good as it would be obtained with a finite difference technique with a relatively large number of nodes, but with less computational cost.

Assuming constant specific heat for the fuel rod materials, an energy balance applied to the first (inner) and the second radial nodes of the two-node fuel rod shown in Figure 2 yields:

$$(M_{f1}C_f)\frac{d}{dt}T_1 = V_1 q_c - \dot{Q}_B, \tag{3}$$

$$(M_{f2}C_f + M_c C_c)\frac{d}{dt}T_2 = V_{f2} q_c + \dot{Q}_B - \dot{Q}_w, \tag{4}$$

where, M_f and M_c represent the fuel and cladding masses and C_f and C_c represent the fuel and cladding specific heats. Note that these balance equations are based on the assumptions that the axial heat conduction in both the fuel and the cladding is negligible and that q_c is uniform.

The above expressions are not exact because T_1 and T_2 are not the average temperature in the respective fuel nodes. They represent the temperatures at radial positions r_1 and r_2 respectively. However, r_1 and r_2 are chosen in a way that they represent the radial positions of the nodal volume averaged temperatures at steady-state full power.

One set of the above balance equations are applied to the pair of fuel nodes associated with each fluid control volume. The time derivatives are approximated by first-order backwards finite differences resulting into implicit equations. The core fuel and the fluid models are connected to each other explicitly via the wall heat flux.

Heat Transfer Rates $\dot{Q}_B$ and $\dot{Q}_w$. The assumed temperature profiles in each region of the fuel rod are used to relate the heat transfer rates at the radial fuel nodes interface, $\dot{Q}_B$, and at the rod wall, $\dot{Q}_w$, to the temperatures T_1, T_2, and to the coolant temperature, T_b. It is assumed that these profile shapes hold for both steady-state and transient

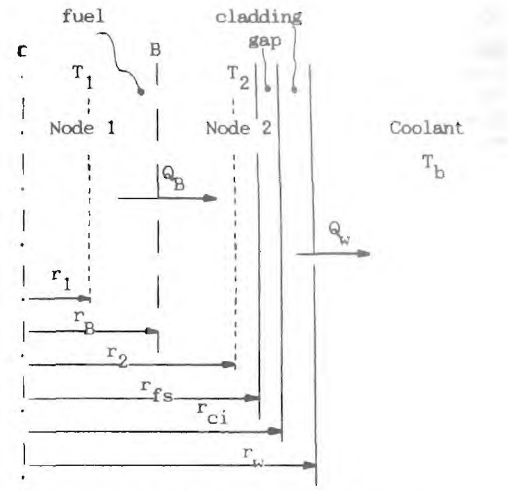

Fig. 2: Schematic of the Two-Node Fuel Rod Spatial Discretization

conditions. For the fuel pellet the temperature profile is assumed to be a parabola and for the cladding a logarithmic function. These profiles are exact for the case of steady-state, uniform heat deposition, and uniform fuel and cladding properties.

The heat transfer rate at the interface, $\dot{Q}_B$, is related to the difference between temperatures T_1 and T_2 by the heat transfer coefficient from radial position r_1 to r_2, U_{12}, given by:

$$U_{12} = \frac{2k_f r_B}{(r_2^2 - r_1^2)}, \tag{5}$$

where k_f is the average fuel thermal conductivity, which is a function of the fuel average temperature.

Two convective heat transfer mechanisms from the rod wall to the coolant are considered, single-phase liquid forced convection and nucleate boiling.

(1) Forced Convection

For the forced convection region the wall heat flux, $\dot{Q}_w$, is related to the difference between temperatures T_2 and T_b through the heat transfer coefficient from radial position r_2 to the coolant, U_{2b}, given by:

$$U_{2b} = \left[\frac{r_w}{2k_{f2}r_{fs}}(r_{fs}^2 - r_2^2) + \frac{r_w}{h_{gap}r_{fs}} + \frac{r_w}{k_c}\ln(r_w/r_{ci}) + \frac{1}{h_{FC}}\right]^{-1}, \tag{6}$$

where k_{f2} is fuel thermal conductivity as function of the fuel temperature in radial node 2, h_{gap} is the gap conductance, k_c is the cladding thermal conductivity, and h_{FC} is the forced convection heat transfer coefficient.

(2) Nucleate Boiling

For nucleate boiling heat transfer the Thom correlation is used. The direct used of this correlation would imply in an iterative solution for the rod temperatures. However, this iteration could have an unacceptable computational cost for a real-time model and so, it is avoided by linearizing the Thom correlation around the wall temperature of the last time step. This method was obtained in [12]. The final solution is given by:

$$\dot{Q}_w^n = \dot{Q}_w^{n-1} + \frac{2\dot{Q}_w^{n-1}}{(T_w^{n-1} - T_{sat}^{n-1})}(T_w^n - T_w^{n-1}), \qquad (7)$$

where the superscript n denotes the time level. The wall temperature at the last time step (at n-1), T_w^{n-1}, is the boiling surface temperature, defined by the Thom correlation with the respective heat flux. Furthermore, the wall temperature can be related to the temperature T_2 by the assumed temperature profile. Thus, the wall heat transfer, $\dot{Q}_w^n$, is expressed in terms of the temperatures T_2 and T_w^{n-1}, as follows:

$$\dot{Q}_w^n = \frac{1}{\eta}\dot{Q}_w^{n-1} + \frac{2\dot{Q}_w^{n-1}}{(T_w^{n-1} - T_{sat}^{n-1})}(T_2^n - T_w^{n-1}), \qquad (8)$$

where η is given by

$$\eta = 1 + \frac{2\dot{Q}_w^{n-1}}{A_w U_{2w}(T_w^{n-1} - T_{sat}^{n-1})}, \qquad (9)$$

and U_{2w} is the heat transfer coefficient from radial position r_2 to the rod surface. The expression for U_{2w} is given by eq. (6) without the term referent to h_{FC}.

Detailed derivations for all these expressions are presented in [7].

Two-Node Fuel Rod Model Evaluation. In the evaluation effort for the heat conduction and convective heat transfer models, the computational code THERMIT-2 [4] was used. This code solves the heat conduction equation in the fuel rod using a finite difference approach. Three different spatial discretizations of the fuel rod were considered for the code THERMIT-2; they are:

. four radial nodes in the fuel rod;
. seven radial nodes in the fuel rod; and
. ten radial nodes is the fuel rod.

In all three cases, one node was used for the gap and one node for the cladding. Different transients were simulated with each one of these three approaches. For these transients a typical PWR fuel assembly was considered. A fixed gap conductance value was used due to limitations of the code THERMIT-2, but variations of fuel and cladding thermal conductivity were considered.

A comparison case for the average fuel temperature is illustrated in Figure 3. The two radial fuel pellet node model (THERMIT-2) is very poor in comparison with the five and eight radial fuel pellet node models (THERMIT-2). The five and eight fuel pellet node model (THERMIT-2) give approximately the same results, indicating that eight nodes are enough to obtain an accurate fuel pellet average temperature for comparison with the two-node model developed. The two-node model developed in this work is seen to be able to predict fuel temperatures that are in good agreement with the eight fuel pellet node model of THERMIT-2.

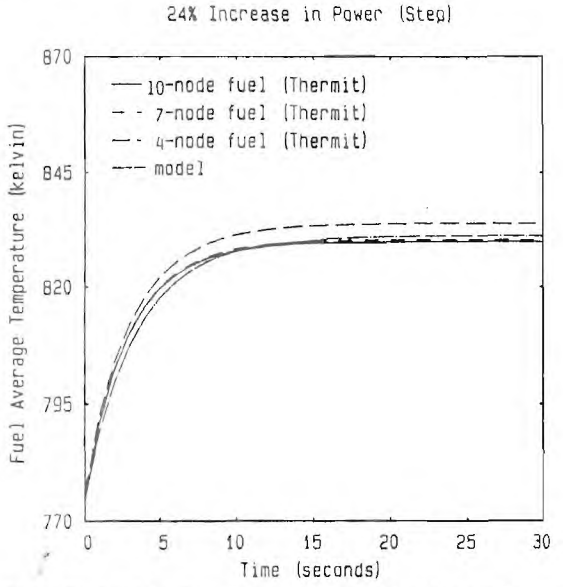

Fig. 3: Fuel Model Transient Verification (Source of Transient: 24% Increase in Reactor Power

Thermal Effects of Fuel Pellet Cracking and Relocation. Pellet cracking and relocation affect significantly the temperature profile in the fuel rod, so that they must be considered if the heat conduction model is to be somewhat accurate. This study adopts and modifies (when necessary) methods developed by others. The results and recommendations of Maki [6] are incorporated to take advantage of the findings of that study.

(1) Gap Conductance:

Before hard pellet-clad contact is made, the total gap conductance, h_{gap}, is determined by the conductance through the gas layer, h_{gas}. The radiation heat transfer through the gap is assumed here to be negligible. To calculate h_{gas} the correlation presented in [13] is used. In this correlation h_{gas} is a function primarily of the gas thermal conductivity and of the inverse of the hot radial gap width (δ). In this study, the variation of thermal conductivity of the gas mixture with temperature is considered, and the hot radial gap incorporates effects such as thermal expansions of fuel and cladding and fuel relocation.

After contact h_{gap} is determined by the contribution of two terms: the conductance through the gas pockets formed between the fuel pellet and cladding surfaces and the contact conductance, h_c. The conductance through the gas pockets is calculated with the same correlation for h_{gas} with δ=0. Contact conductance is also computed as in [13]. In this correlation h_c is a major function of the contact pressure between the fuel and the cladding. The pellet-clad contact pressure used here is derived from an elastic analysis [6]. The stresses then are only correct for short duration intervals of heat rates above that for initial contact. If the intervals are too long or if the heat rate too high then inelastic processes, creep and/or plasticity cause the contact

pressure to be reduced. However, these refinements have been excluded here not only for simplicity but also because the gap temperature rise is usually small in such cases and the temperature errors correspondingly small.

(2) Thermal Strain and Hot Gap Width

Thermal strains of the fuel and cladding are the primary parameters that affect the gap width. Approximating the logarithmic temperature profile adopted for the cladding by a linear function, the average cladding thermal strain is given by the following:

$$\bar{\epsilon}_{Tc} = \epsilon_{Tc}(T_c), \tag{10}$$

where ϵ_{Tc} is the cladding thermal strain as function of the temperature and T_c is the average cladding temperature.

The hot inside cladding radius is then given by cold inside cladding radius plus the correction due to the thermal strain. The cold inside cladding radius is obtained from the as fabricated value plus a correction due to cladding creepdown. Note however, that cladding creepdown is not directly incorporated into the model. It can be provided as external input, and it is then indirectly incorporated by adjusting the cold inside cladding radius.

It should be noted that elastic deformation of the cladding, due to the difference between the coolant pressure and the internal rod pressure, is not considered.

The average fuel thermal strain is approximated by the thermal strain associated with the radial fuel rod node temperatures, T_1 and T_2, as follows:

$$\bar{\epsilon}_{Tf} = b_1\epsilon_{Tf}(T_1) + b_2\epsilon_{Tf}(T_2), \tag{11}$$

where ϵ_{Tf} is the fuel thermal strain as function of the temperature, and b_1 and b_2 are constants used to calculate the average fuel temperature as function of T_1 and T_2. These constants are obtained from a steady-state analysis, their derivation is presented in ref. [7].

The hot fuel pellet radius is then determined by the cold fuel pellet radius plus the correction due to the thermal strain. The cold fuel pellet radius is calculated from the nominal as fabricated radius plus corrections due to fuel densification, fuel swelling, and fuel relocation. The correction due to relocation is directly incorporated into the model. Fuel densification and swelling are not directly taken into account by the model. However, they can be provided as external input and they are then indirectly incorporated by adjusting the cold fuel pellet radius.

The radial gap width is the difference between the inside cladding radius and the outside pellet radius.

(3) Fuel Pellet Relocation

There are many methods of incorporating relocation into the fuel temperature calculation. In this study the method of ref. [14] was adopted. In this method the increase of pellet radius due to relocation, Δr_{reloc}, is a function of the cold radial gap width.

Another treatment considered in this study is that of no relocation. In this case Δr_{reloc} is always set equal to zero and the fuel pellet conductivity is found on an uncracked basis. This model is used as a reference case for the evaluation of the solid pellet relocation model.

(4) Fuel Conductivity

Two major factors affect the fuel thermal conductivity: porosity of the sintered UO_2 and fuel cracking. The porosity is taken into account by a porosity factor (PF) [15].

Fuel cracking has to be considered together with fuel relocation. For cracked fuel pellets, the reduction in heat transfer due to cracks within the fuel is accounted for by an effective fuel thermal conductivity. The effective conductivity is defined as,

$$k_f = (CCF)(PF)k_{UO_2}, \tag{12}$$

where k_{UO_2} is the UO_2 thermal conductivity, and CCF is the cracked fuel conductivity correction factor. The correlation used for this correction factor is taken from [14], the same source of the solid fuel relocation model. This factor is a function of many variables and among them the hot gap width. In the original correlation for CCF the hot radial gap does not consider the change in fuel radius due to relocation. The hot radial gap incorporates then, only thermal expansion of the fuel and clad over the initial cold gap. A modification of this treatment is adopted here by using a hot radial gap that besides thermal expansion incorporates fuel swelling, fuel relocation, and cladding creepdown. This was done in order to improve the correlation with experimental results for fuel center-line temperature. However, to illustrate this modification, both cases were evaluated using experimental data.

Finally, note that fuel restructuring, which may lead to crack healing, is not considered in the model.

Evaluation of Gap Conductance and Thermal Effects Models. The fuel relocation/cracking and gap conductance model during steady state was validated against 250 experimental values of fuel center line temperature from [14], [15], [16] and [17], and 39 experimental data of fuel surface temperature from [14]. Note that three other models for fuel relocation and cracking were also tested; the methods of ref. [14] (note that a modified version of these methods were adopted), a model without relocation and cracking, and the methods of ref. [17] (test performed by Maki [6]). A summary of the results is presented in Table 3. In this table the adopted method is indicated as "adopted", the methods of ref. [14] as "Ref. [14]", the no relocation and cracking model as "no relocation" and the methods of ref. [17] as "Maki [6]".

Table 3
Summary of Relocation/Cracking Validation

Temperature	Model	Average Error (^{o}C)	Standard Deviation (^{o}C)
Fuel Surface	No Rel.	25	38
	Adopted	-31	25
	Maki [6]	-59	-
Center-line	No Rel.	64	65
	Adopted	2	80
	Ref.[14]	135	-
	Maki [6]	78	-

Note: Errors indicate calculated minus experimental.

None of the models is perfect in predicting the whole range of experimental data for both fuel center

line temperature and fuel surface temperature. However, it can be observed that the adopted method is the one more capable of giving meaningful results for average fuel temperature. All the other methods tend to overpredict this temperature. The statistical nature of the phenomena involved gives a large data scatter. This nature combined with the small number of data points, in the case of fuel surface temperature gives an extra uncertainty to the statistical measures listed. For the results of fuel center line temperature the large standard deviation has to be seen as a consequence of this statistical nature of the phenomena.

Note that all of these experiments are at relatively low burnup. Therefore the treatment of swelling, creepdown, and other lifetime effects are not directly validated.

MODEL EVALUATION

The final step in the model development is validation. Partial evaluations were performed: the subcooled vapor fraction model, and the fuel relocation and cracking model were checked against experimental results; the two radial fuel node model was check using results from the computational code THERMIT-2 [4].

During many existing modes of PWR operation, turbine generator conditions are defined by operating personnel. The core is then controlled to maintain specific primary temperature values. Therefore, in simulating real plant data, it is important to model primary loops and steam generators and to couple these models to the core model. Simple models are used for these components. Details about these models can be obtained in [7]. This complete plant model is validate over different transient conditions, including load rejection, load step, load reduction, and a power ascension from zero to full power. The results of the validation effort are encouraging, indicating that the models are suitable for application to any operational transient.

Figures 4 presents the main results of a power ascension transient from zero to full power. Some of the calculated values are presented as an error from the experimental value; the error is the calculated minus the experimental. It can be seen that the model describes the experimental results very well. The calculated steam pressure shows a bias; possible causes include pressure measurements errors, errors in the geometric or heat transfer parameters, and error in the fouling factor for the outside surface of the steam generator tubes. From the steam generator pressure it can be seen that the calculated value shows more noise than the experimental value (the same is true for the other parameters). The source of this noise increase is that the experimental data, which is noise, is sampled every 30 seconds and so extremes persist long enough to cause an excess plant reaction.

Equally important as the validation step is the execution speed of the computer model. Real time

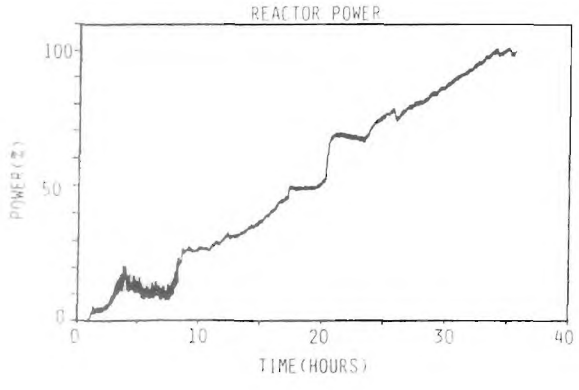

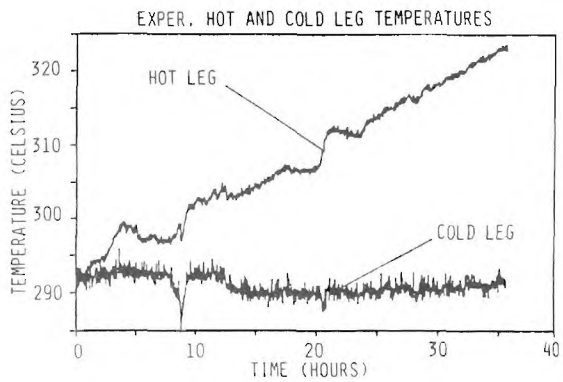

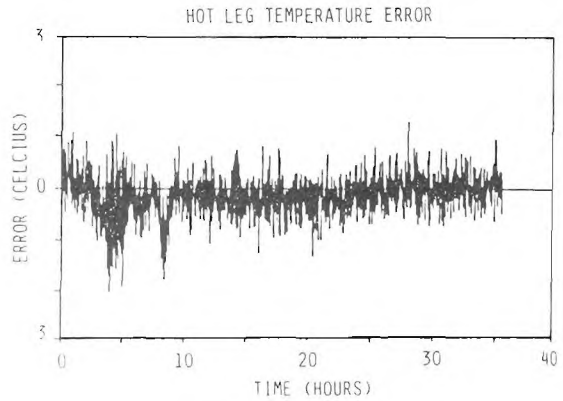

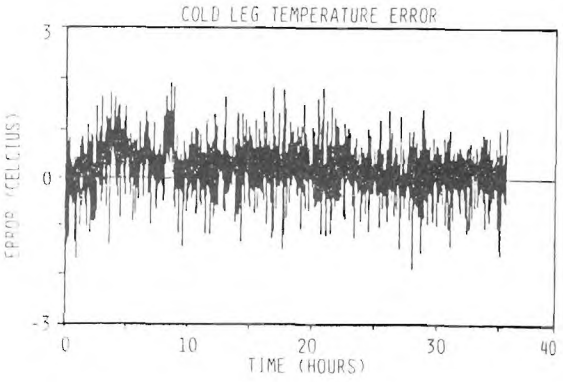

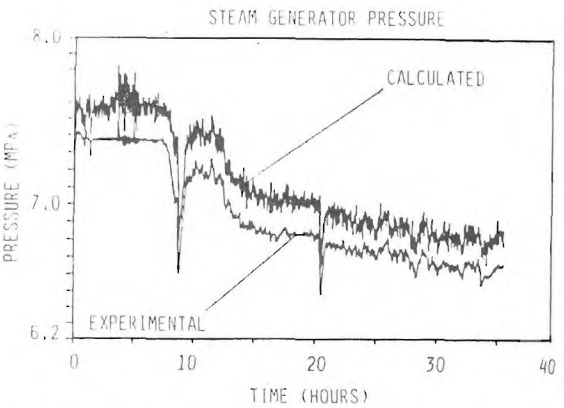

Fig. 4: Simulation Results of Power Ascension Transient

execution can be achieved with 74 control volumes in the core and one primary loop if a time step size of 2 seconds is used. This result was obtained on a personal computer equipped with microprocessors Intel 8088/8087

running at 8 MHz.

CONCLUSIONS

A description has been given of a fast running model that provides three-dimensional thermal-hydraulic information for a PWR core. The model describes in detail both fuel and coolant conditions and is coupled with models for primary loop and steam generator. These models produce an analytic toll that can be applied not only in a power/power distribution controller but also directly to other aspects of operation of a commercial PWR. They can be used, for instance, as a simulation tool or incorporated is a SPDS. The model was validated during operational transients with encouraging results and the execution speed was checked. Finally, note that the features of the core model developed will only be totally used after the coupling of this model with a real-time three dimensional neutronic model.

REFERENCES

[1] P. W. Kao, "Application of Super-Nodal Methods to Transient Analysis," Ph.D. Thesis, Dept. of Nucl. Eng., M.I.T., Ago. 1988.

[2] S. P. Kao , "A Multiple-Loop System Model for Pressurized Water Reactor Plant Sensor Validation," Ph.D. Thesis, Dept. of Nucl. Eng., M.I.T., July 1984.

[3] C. W. Stewart et al., "COBRA-IV: The Model and the Method," BNWL-2214, July 1977.

[4] J.E. Kelly, S.P.Kao and M.S. Kazimi, "THERMIT-2: A Two Fluid Model For Light Water Reactor Subchannel Transient Analysis," MIT Energy Laboratory, 1981.

[5] C. Chiu, "Three-Dimensional Transport Coefficient Model and Predictor-Correction Numerical Method for Thermal Margin Analysis of PWR Cores," Nucl. Eng. and Design, 64, 103-115, 1981.

[6] J. T. Maki, "Thermal Effects of Fuel Pellet Cracking and Relocation," MS Thesis, Dept. of Nucl. Eng., M.I.T., 1979.

[7] E. L. Cabral, "Real-Time Three Dimensional Thermal-Hydraulic Model and Non-Linear Controller for Large PWR Cores," Ph.D. Thesis, Dept. of Nuclear Eng., M.I.T., Nov. 1988.

[8] Northeast Utility Co., "Millstone Nuclear Power Station - Unit 3: Final Safety Analysis Report.

[9] G.W. Maurer, "A Method of Predicting Steady State Boiling Vapor Fraction in Reactor Coolant Channels," WAPD-BT-19, 1960.

[10] R.A. Egen, D.A. Dengee and J.W. Chastian, "Vapor Formation and Behavior in Boiling Heat Transfer," BMI-1163, 1957.

[11] P. Martin, "Measurement of Local Void Fraction at High Pressure in a Heating Channel," Nuclear Science and Engineering, 48, 125, 1972.

[12] J. E. Meyer and J. S. William Jr., "A Momentum Integral Model for the Treatment of Transient Fluid Flow," WAPD-BT-25, 1965.

[13] G. E. Beyer et al., "GAPCON-THERMAL II: A Computer Program for Calculating the Thermal Behavior of an Oxide Fuel Rod," BNWL-1898, Nov. 1975.

[14] R.W. Garner, D.T. Sparks, R.H. Smith, P.E. Klink, D.H. Schweder and P.E. MacDonald, "Gap Conductance Test Series-2, Test Results Report for Tests GC2-1, GC2-2, and GC2-3," TREE-1268, 1978.

[15] G. Kjaerheim and E. Rolstad, "In-Pile Determination of UO2 Thermal Conductivity, Density Effects, and Gap Conductance," HPR-80, 1979.

[16] E. T. Laats, P. E. MacDonald and W. J. Quapp, "USNRC-OECD Halden Project Fuel Behavior Test Program, Experimental Data Report for Test Assemblies IFA-226 and IFA-239," ANCR-1279, 1970.

[17] P. E. MacDonald and J. M. Broughton, "Cracked Pellet Gap Conductance Model: Comparison of FRAP-S Calculations with Measured Fuel Centerline Temperatures," CONF-750360-2, 1975.